SUMOylation and deimination of proteins: Two epigenetic modifications involved in *Giardia* encystation

Cecilia V. Vranych [a,1], María R. Rivero [a,1], María C. Merino [a,1], Gonzalo F. Mayol [a,1], Nahuel Zamponi [a,1], Belkys A. Maletto [b,1], María C. Pistoresi-Palencia [b,1], María C. Touz [a,1], Andrea S. Rópolo [a,*,1]

[a] *Laboratorio de Microbiología e Inmunología, Instituto de Investigación Médica Mercedes y Martín Ferreyra, INIMEC–CONICET, Universidad Nacional de Córdoba, Friuli 2434, 5000 Córdoba, Argentina*
[b] *Departamento de Bioquímica Clínica, CIBICI–CONICET, Facultad de Ciencias Químicas, Haya de la Torre y Medina Allende, UNC, 5000 Córdoba, Argentina*

ABSTRACT

SUMOylation, a posttranslational modification of proteins, has been recently described as vital in eukaryotic cells. In a previous work, we analyzed the role of SUMO protein and the genes encoding the putative enzymes of the SUMOylation pathway in the parasite *Giardia lamblia*. Although we observed several SUMOylated proteins, only the enzyme Arginine Deiminase (ADI) was confirmed as a SUMOylated substrate. ADI is involved in the survival of the parasite and, besides its role in ATP production, it also catalyzes the modification of arginine residues to citrulline in the cytoplasmic tail of surface proteins. During encystation, however, ADI translocates to the nuclei and downregulates the expression of the Cyst Wall Protein 2 (CWP2). In this work, we made site-specific mutation of the ADI SUMOylation site (Lys101) and observed that transgenic trophozoites did not translocate to the nuclei at the first steps of encystation but shuttled in the nuclei late during this process through classic nuclear localization signals. Inside the nuclei, ADI acts as a peptidyl arginine deiminase, being probably involved in the downregulation of CWPs expression and cyst wall formation. Our results strongly indicate that ADI plays a regulatory role during encystation in which posttranslational modifications of proteins are key players.

© 2014 Elsevier B.V. All rights reserved.

1. Introduction

An interesting feature of parasites is their ability to rapidly and efficiently adapt to changes of the environment in order to survive. A dynamic survival mechanism is used by *Giardia lamblia* (syn. *Giardia duodenalis*, *Giardia intestinalis*), a parasitic protozoan early divergent in evolutionary history and a major cause of waterborne diarrheal disease [1,2]. The life cycle of *Giardia* is simple, but sufficient to adapt to the microenvironment, with two clearly different stages adapted to survive outside (cysts) or inside (trophozoites) the host.

Cysts are covered by a wall composed of proteins (CWPs: Cyst Wall Proteins) and a glycopolymer in insoluble fibrils [3]. This extracellular wall permits the parasite to survive in the environment, where it may persist in fresh water and also resist disinfectants. Transmission of *Giardia* is via the fecal–oral route, either indirectly through contaminated water or food, or directly from person to person [2]. After ingestion and exposure to the acidic environment of the host's stomach, cysts rapidly

differentiate into vegetative trophozoites via the excyzoite stage. The excyzoite divides twice giving rise to trophozoites, which attach to the intestinal epithelium with an adhesive disk in order to proliferate and to avoid being swept away with the intestinal content. To evade the host's immune response, it changes its surface proteins (VSPs: Variant-specific Surface Proteins) in a process called antigenic variation. In the lower part of the small intestine, and in response to host signals, the trophozoites encyst. Synthesis of CWPs begins early in encystation and leads to the formation of novel large encystation secretory vesicles (ESVs), which export CWPs to the nascent cyst wall. The late phase of encystations consists in the secretion of cyst wall material to the parasite surface, followed by the assembly of the filamentous portion of the cyst wall.

In parasites, efficiency to react to changes in the microenvironment is directly related to their survival odds. Posttranslational protein modifications enable cells to rapidly and specifically respond to endogenous or exogenous stimuli, avoiding time- and energy-consuming de novo protein synthesis. In eukaryotic cells, modifications of arginine residues by deimination (protein citrullination) are catalyzed by peptidyl arginine deiminases (PADs), generating irreversible structural modifications of protein by the conversion of arginine residues to citrulline residues. Because no citrulline tRNA exists, the presence of citrulline residues in proteins has to be the result of posttranslational modifications (reviewed in [4]).

---

* Corresponding author at: Instituto de Investigación Médica Mercedes y Martín Ferreyra, Friuli 2434, 5000 Córdoba, Argentina. Tel.: +54 351 4681465; fax: +54 351 4695163.
E-mail address: aropolo@immf.uncor.edu (A.S. Rópolo).
[1] Tel.: +54 351 468 1465; fax: +54 351 4695163.

In *Giardia*, we previously showed that the enzyme Arginine Deiminase (ADI), besides its role as a metabolic enzyme converting free L-arginine into L-citrulline, is able to act as a PAD. During the proliferative stages of growth, ADI was observed to deiminate and convert the arginine of the conserved cytoplasmic tail of VSPs to citrulline, a modification that is important in the regulation of antigenic variation [5]. The change of one VSP into another allows the parasite to evade the humoral immune response and to prolong infections within the host. There is another way by which *Giardia* trophozoites are involved in the inhibition of the immune response applied by the host. It has been demonstrated that ADI, enolase, and ornithine carbamoyl transferase (OCT) enzymes are released into the medium when the trophozoite is in contact with intestinal epithelial cells in vitro [6]. The presence of ADI and OCT in the gut lumen may contribute to L-Arg depletion, and finally impact the availability of free L-Arg to be used for the production of nitric oxide by intestinal epithelial cells (reviewed in [7]). Also, a growth arrest of intestinal epithelial cells, changes in the surface markers and cytokine response of in vitro-activated human monocyte-derived dendritic cells and impaired T cell proliferation are affected due to reduced arginine availability [8–10]. All this, and the fact that ADI is an essential enzyme for *Giardia* survival indicate that ADI is a potential target for the development of therapeutic agents for the treatment of giardiasis [11].

ADI translocates to the nuclei late during the encystation process, suggesting a role during the differentiation of cysts. Translocation of ADI to nuclei takes place early in ADI-transgenic cells, in which the high overexpression of ADI together with its nuclear translocation avoids CWP2 expression [5]. Therefore, probably ADI causes genes in the CWP family to turn off, as an essential requirement to successfully complete the encystation stage.

Numerous studies have shown that, in eukaryotic cells, nuclear proteins or proteins that crisscross the nuclear membrane contain a stretch of basic amino acid sequence known as the Nuclear Localization Signal (NLS). Proteins with a NLS are transported across the nuclear envelope by a family of transport proteins called importins. In addition, nucleocytoplasmic transport is modulated by posttranslational modification of the cargo protein, including phosphorylation, acetylation and SUMOylation, which could mask or expose the NLS of the protein. SUMOylation is characterized by the covalent attachment of SUMO (Small Ubiquitin-related MOdifier) proteins to specific lysine residues in target proteins [12,13]. The molecular weight of SUMO is approximately 11 kDa, which usually generates a rise in the molecular weight of the target protein. We previously demonstrated that the translocation of ADI from the cytoplasm to the nuclei and the increased M_r observed in nuclear fractions of encysting cells may be explained by SUMOylation of the enzyme [5]. Moreover, recently, we disclosed the presence of a single gene in *Giardia* (*gsumo*) that encodes the SUMO protein, and identified genes encoding putative enzymes of the SUMOylation pathway [14].

The present study focuses on the role of ADI during encystation of *Giardia*, and describes the function of the enzyme inside the nuclei. Furthermore, we analyze how SUMOylation of the enzyme influences its translocation to the nuclei and consequently its participation in the modulation of cyst differentiation in *Giardia*.

2. Materials and methods

2.1. Biochemical reagents

Unless otherwise stated, all chemicals were purchased from Sigma (St. Louis, MO).

2.2. Parasites

Trophozoites of the isolate WB, clone 1267 (WB/1267) (American Type Culture Collection catalog number 50582) were cultured in TYI-S-33 supplemented with 10% fetal bovine serum and bovine bile for 48 h at 37 °C [15]. Cultures were harvested by chilling on ice followed by agitation to dislodge attached cells. Trophozoites were collected by centrifugation at 500 g for 10 min at 4 °C and washed three times with PBS. Trophozoites of the WB/1267 clone were transfected by electroporation and selected with puromycin [16,17]. A two-step encystation procedure was used by increasing the medium pH and by addition of porcine bile as reported by Boucher and Gillin [18].

2.3. Expression of ADI, ADI variants and SUMO in WB/1267 trophozoites

To predict the SUMOylation sites, SUMOsp 2.0 [19] and the PCI-SUMO (from the Department of Systems and Computer Engineering from Carleton University) programs were used. The Quik Change Mutagenesis Kit (Stratagene) was used to introduce point mutations in the SUMOylation site of the *adi* gene. The sequences of the primers were: ADIK101A-HAF: 5′-gcaatggcctcgctggcgtacgagctccatgc-3′ and ADIK101A-HAR: 5′-gcatggagctcgtacgccagcgaggccattgc. Point mutations in the sites of the nuclear localization signals were introduced using the following primers: mNLS1F: 5′-gaccagcagataaccaccgcggcgggaa tagtcatgggccag-3′ and mNLS1R: 5′-ctggcccatgactattcccgccgcggtggttat ctgctggtc-3′; mNLS2F: 5′-accacccggcgcggaatagcggcgggccagtttcaggc-3′ and mNLS2R: 5′-gcctgaaactggcccgccgctattccgcgccgggtggt-3′; mNLS3F: 5′-cagtttcaggcggcgcagaggaggc-3′ and mNLS3R: 5′-gcctcctctgcgccgcctg aaactg-3′. The entire open reading frame of each mutant gene was sequenced to ensure that the appropriate mutation was obtained without incorporation of undesired mutations (Macrogen). To constitutively express ADI (*ADI-HA* cells), mNLS and ADIK101A (*ADI$_{K101A}$-HA* cells), the plasmid pTubHApac with HA at the C-terminus was employed [20] *SUMO-HA* transfected cells were expressed as previously described [14]. The vectors contain a puromycin cassette under the control of the endogenous non-regulated tubulin promoter for cell selection. Stable trophozoite transfection was performed as previously described [16, 17,21–23]. Drug resistant trophozoites were usually apparent by 7–10 days post transfection.

2.4. Immunofluorescence

Cells were washed with PBSm (1% growth medium in PBS, pH 7.4), allowed to attach to multiwell slides in a humidified chamber at 37 °C for 1 h, and the wells were fixed with fresh 4% formaldehyde for 40 min. The cells were incubated sequentially with blocking solution (10% goat serum and 0.1% Triton X-100 in PBS) at 37 °C for 30 min and incubated with the specific mAb (1:300) in PBS containing 3% normal goat serum and 0.1% Triton X-100 for 1 h at 37 °C, followed by incubation with FITC-conjugated goat anti-mouse (1:200) secondary antibody (Cappel Laboratories) at 37 °C for 1 h. For double staining, FITC or Texas red conjugated anti-HA mAb (1:100) (Sigma, St. Louis, MO) to detect HA-tagged proteins, and polyclonal Ab against ADI (1:800) (kindly provided by A. Hehl) or anti-SUMO (13C5) monoclonal Ab (1:100) (mAb) [14], followed by incubation with FITC or Texas Red-conjugated goat anti-mouse antibody (1:200) (Cappel Laboratories), were used. FITC-conjugated anti-CWP1 mouse mAb (1/200) (Waterborne, New Orleans, LA, USA) was also used. Control with non-related antibodies was included. Finally, preparations were washed and mounted in Vectashield mounting media. Images were collected on Olympus FV1000 confocal microscope using 63× oil-immersion objectives (NA 1.32, zoomX). Fluorochromes were excited using an argon laser at 488 nm for FITC and a krypton laser at 568 nm for Texas Red. Detector slits were configured to minimize any crosstalk between the channels. Differential Interference Contrast (DIC) images were collected simultaneously with the fluorescence images by use of a transmitted-light detector. Images were processed using ImageJ and Adobe Photoshop 8.0 (Adobe Systems) software. For quantitative studies, all images of a given experiment were exposed and processed identically. At least 70–100 cells expressing each type of protein were examined. The data were statistically evaluated using Student's *t* test.
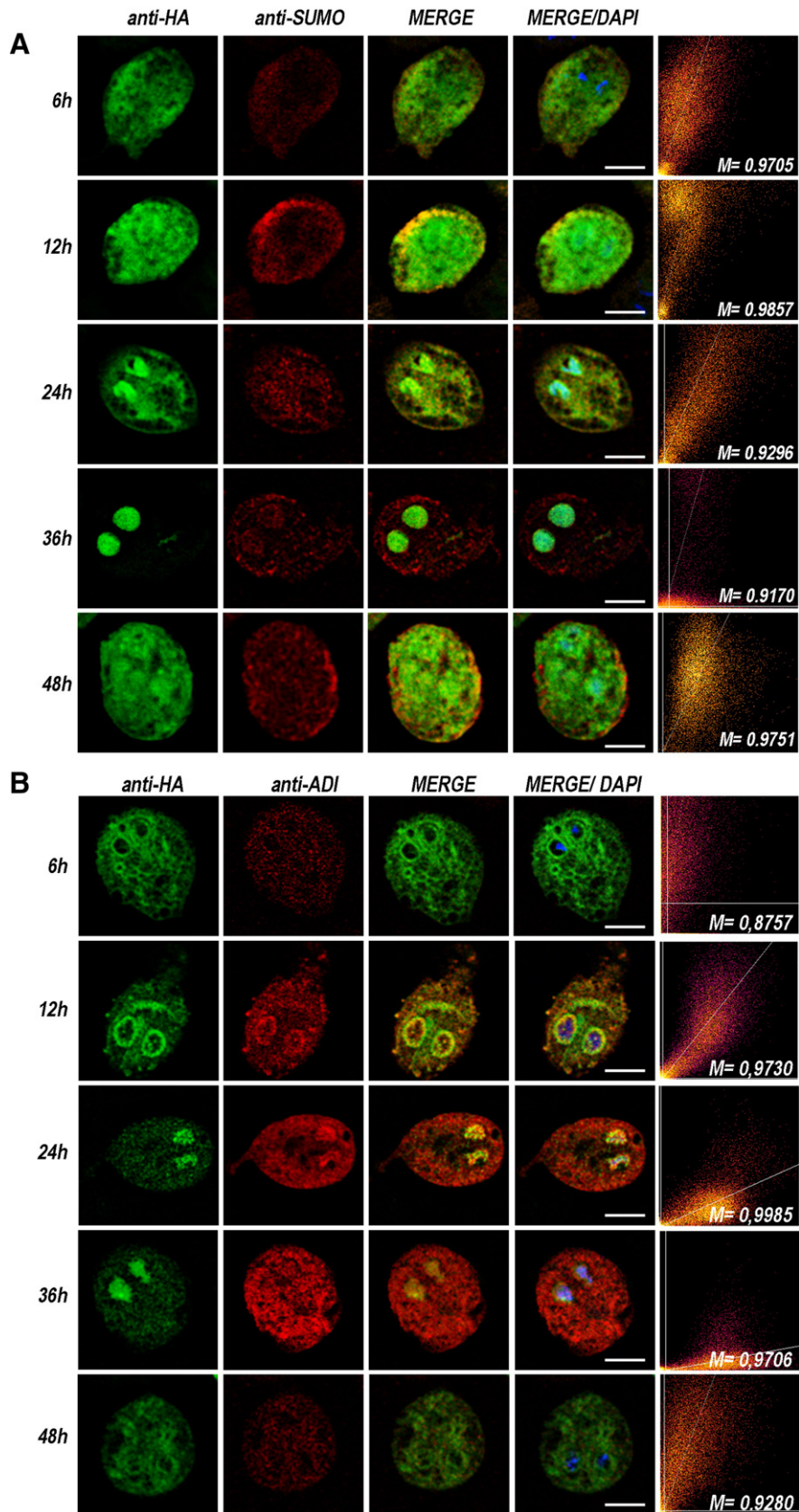
Fig. 1. ADI is a SUMOylated enzyme. A) Direct IFA and confocal microscopy on permeabilized cells at different points after induction of the encystation process shows a cytoplasmic and nuclear distribution of ADI-HA (green) by using FITC-labeled anti-HA mAb. ADI-HA partially colocalizes (yellow merge) with SUMO (red) detected by using an anti-SUMO mAb (13C5). Nuclear DNA was labeled with DAPI (blue). The scatter plots of the two labels show the colocalization. Mander's overlap coefficient (M). Bars, 3 μm. B) *SUMO-HA* transgenic cells were used to analyze the localization of ADI. Anti-HA mAb was used to detect SUMO-HA in transgenic cells (green). ADI was detected using a specific polyclonal antibody (red). Partial colocalization (yellow merge) with ADI was observed. Nuclear DNA was labeled with DAPI (blue). The scatter plots of the two labels show the colocalization. Mander's overlap coefficient (M). Bars, 3 μm.
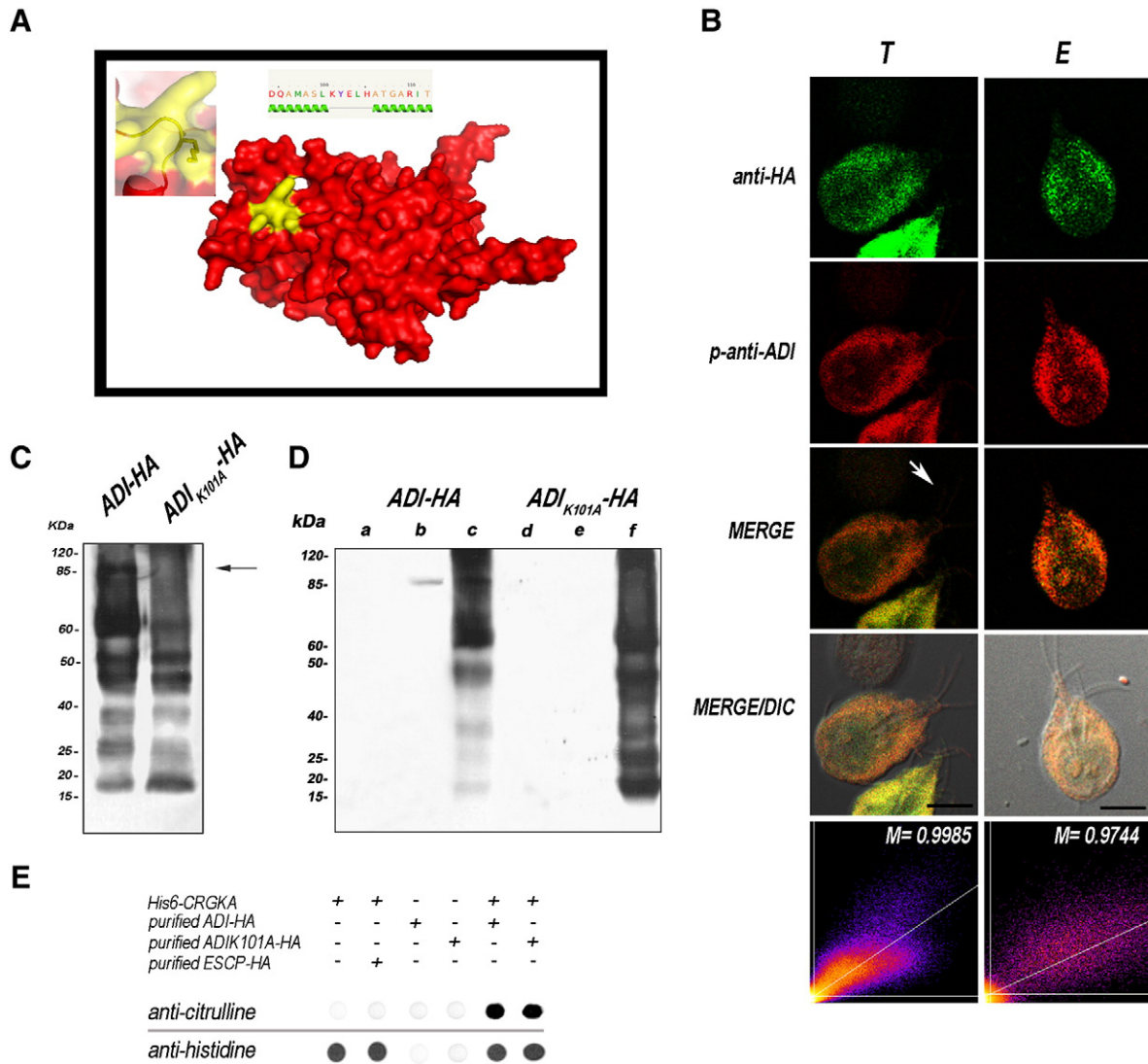
Fig. 2. SUMOylation site in ADI. A) 3D model of ADI built with the web server Phyre2 to predict ADI protein structure. Residues of the SUMOylation motif are in yellow. This figure was prepared using the PyMOL program (DeLano Scientific, USA). Secondary structure of ADI is also represented showing that the Lys101 (K101) is located in a loop flanked by two helixes with Lys101 (K101) clearly exposed. B) IFA and confocal microscopy on permeabilized ADI_{K101A}-HA transgenic cells labeled with FITC-conjugated anti-HA mAb (green). Native and transgenic ADI is labeled with Texas Red-conjugated anti-ADI pAb (red). There is a strong colocalization in cytoplasm (yellow merge) both in growing and encysting trophozoites. Flagellar staining is observed in growing trophozoites (arrow). The scatter plots correspond to the colocalization analysis. Mander's overlap coefficient (M). DIC (differential interference contrast) microscopy is shown. Bars, 3 μm. C) Western blotting performed during encystation (36 h) using anti-HA mAb in ADI-HA and ADI_{K101A}-HA transgenic cells shows multiple bands. An increase in molecular mass from a 64–66 kDa to an 85 kDa band is shown (black arrow). Absence of 85 kDa band corresponding to the SUMOylated ADI form is observed in ADI_{K101A}-HA cells. Line 1: M_r: Relative Molecular Mass (kDa). D) Western blotting using HRP-conjugated anti-HA mAb was performed to detect ADI bands after immunoprecipitation with anti-SUMO mAb (13C5) in ADI-HA (a, b, and c) and ADI_{K101A}-HA transgenic cells (d, e, and f) 36 h after the induction of the encystation process. (a and d) Control using a non-related antibody; (b and e) anti-SUMO mAb; (c and f) ADI in lysate before IPP. E) Dot-blotting to detect citrullination of the His_6-CRGKA peptide after incubation with purified enzymes ADI-HA and ADIK101A-HA. A non-related purified enzyme ESCP-HA was used as a negative control. Dot blotting to detect His_6-CRGKA was performed using anti-H_6 mAb.

2.5. Quantitative colocalization analysis (QCA)

Confocal immunofluorescence microscopy and quantitative colocalization analysis were performed using Fiji image processing package (http://fiji.sc/wiki/index.php/Fiji). Background was corrected using the threshold value for all channels to remove background and noise levels completely. The Mander's (M) overlap coefficient was examined. The M values range from 0 to 1.0. If the image has an overlap coefficient of 0.5, it implies that 50% of both its objects, i.e. pixels, overlap. A value of zero means that there are no overlapping pixels. This coefficient is not sensitive to the limitations of typical fluorescence imaging [24–27]. Colocalization is considered in the range from 0.7 to 1.0.

2.6. Flow cytometry analysis

For the evaluation of the completion of the encystation process, trophozoites were grown to a monolayer in pre-encysting media and induced to encyst as described below. After 36 h, encysting cells and cysts were harvested by chilling on ice followed by centrifugation at 500 g for 10 min at 4 °C. To analyze stain cell surface expression of CWPs (cysts), cells were washed with PBS and stained with FITC-labeled anti-CWP1 (1:100 in PBS) for 1 h at 4 °C. After washing three times with PBS, cells were fixed in 4% paraformaldehyde. Controls included the use of an unrelated antibody. Cells were analyzed on a Cytoron Absolute Cytometer (Ortho Diagnostic System). Data were analyzed using FlowJo Analysis Software.
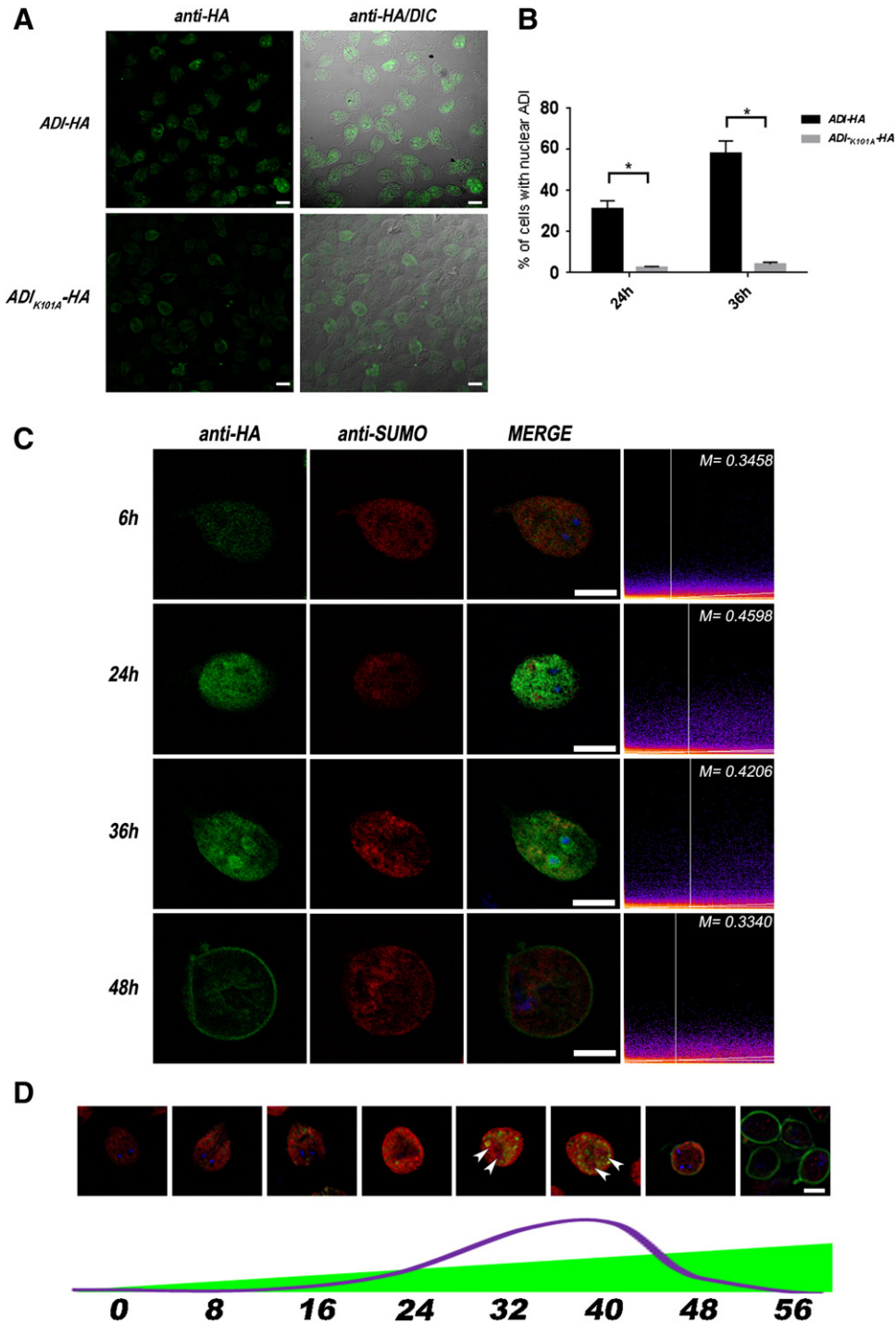
Fig. 3. Entry of ADI to nuclei is enhanced by SUMOylation of the enzyme. A) IFA and confocal microscopy shows the localization of ADI in the cytoplasm and nuclei in *ADI-HA* encysting cells (36 h) but mainly in the cytoplasm of mutated trophozoites (*ADI$_{K101A}$-HA*). Right panels show the differential interference contrast (DIC) images. Scale bar, 10 μm. B) Quantification of cells presenting nuclear transgenic ADI (presented as a percentage of total counted transfected cells) at 24 or 36 h after induction of the encystation process showed a significant reduction in nuclear localization in *ADI$_{K101A}$-HA* compared with *ADI-HA* transgenic cells. Data represents the means ± s.d. of three independent experiments, *p < 0.05. C) Confocal microscopy of IFA in encysting *ADI$_{K101A}$-HA* trophozoites shows no colocalization between ADIK101A-HA and the giardial SUMO at different times during the encystation process. ADIK101A-HA was labeled with FITC-conjugated anti-HA mAb (green) while gSUMO was labeled with Texas Red-conjugated anti-SUMO (13C5) mAb (red). Nuclei were stained with DAPI (blue). Scale bar, 10 μm. The scatter plots (lower panels) correspond to the colocalization analysis. Mander's overlap coefficient (M). D) Kinetics of the encystation process (0, 8, 16, 24, 32, 40, 48, and 56 h) to analyze the localization of *ADI$_{K101A}$-HA* transgenic cells. ADIK101A-HA was labeled with Texas Red-conjugated anti-HA mAb (red); CWP1 was labeled with FITC-conjugated anti-CWP1 mAb (green). Nuclei were stained with DAPI (blue). Localization of ADIK101A-HA in nuclei is indicated (arrow). Scale bar, 3 μm. In the lower part, a diagram of the process is drawn showing the increase of CWP (green) and the kinetics of the localization of the enzyme in the nuclei (violet).

2.7. Western blotting

Total protein (20 μg) from parasite lysates were harvested and incubated with sample buffer and protease inhibitors, boiled for 10 min and separated on 12% Bistris gels. Samples were transferred to nitrocellulose membranes, blocked with 5% skimmed milk and 0.05% Tween 20 in TBS, and incubated with anti-HA mAb (1/1000) diluted in the same buffer. After incubation with horseradish peroxidase-conjugated polyclonal

Table 1
In silico prediction of nuclear localization. The different mNLS mutants used in the present study are shown. The mutated residues are indicated in gray.

	Sequence	NLSs	
		RRGIVMGQFQAPQRRRE	PQRRREQ
NLS	RRGIVMGQFQAPQRRREQ	Bound	Bound
mNLS1	AAGIVMGQFQAPQRRREQ	Not bound	Bound
mNLS2	RRGIAAGQFQAPQRRREQ	Bound	Bound
mNLS3	RRGIVMGQFQAAQRRREQ	Bound	Not bound

goat anti-mouse Igs (1/1000) (Dako), proteins recognized by antibodies were visualized with autoradiography. Controls included the use of an unrelated antibody.

2.8. Immunoprecipitation assays

Giardia trophozoites were harvested and disrupted in lysis buffer (50 mM Tris, pH 8.0, 120 mM NaCl, 5 mM EDTA, 1% Triton X-100, and protease inhibitors) for 30 min on ice and centrifuged at 13,000 g for 5 min at 4 °C. The cell lysate was precleared by using protein A/G-Sepharose beads (Santa Cruz Biotechnology, Santa Cruz, CA) for 30 min at 4 °C, and subsequently subjected to immunoprecipitation by using 300 μl of anti-SUMO mAb (13C5). After incubation overnight at 4 °C, protein L-agarose was added, and the incubation was continued for 4 h. Beads were pelleted at 700 g and washed four times with wash buffer (50 mM NaH$_2$PO$_4$, 300 mM NaCl pH 8.0, 0.1% Triton X-100, and protease inhibitors). Beads were suspended in sample buffer and boiled for 10 min before Western blot analysis.

2.9. Citrullination assay

For IFA of fixed cells, trophozoites were cultured in encysting medium and were harvested after 36 h of encystation. Citrullinated proteins were detected by using the anti-citrulline (modified) detection kit (Upstate) as previously described [28]. Controls included omission of the anti-citrulline antibody or absence of the chemically modifying citrulline step. Preparations were mounted in Vectashield mounting media. Images were collected on an Olympus FV1000 confocal microscope using 63× oil-immersion objectives (NA 1.32, zoomX). Differential interference contrast (DIC) images were collected simultaneously with the fluorescence images by use of a transmitted-light detector. Images were processed using ImageJ and Adobe Photoshop 8.0 (Adobe Systems) software.

2.10. ADI activity

ADI activity was assayed by measuring the modification of His6-CRGKA peptide to His6-CcitGKA as we previously described [5]. Briefly, trophozoites expressing ADI-HA, ADIK101A-HA, mNLS1, mNLS2,

mNLS3 and ESCP-HA [22] were cultured, collected and sonicated in PBS buffer at 4 °C until there were no intact cells and centrifuged at 700 g for 10 min. All HA-tagged proteins from transfected trophozoites were purified using anti-HA and protein A/G-agarose as previously described [22]. 5 mM of soluble His$_6$-CRGKA peptide (10 mg/ml of peptide in ADI activity buffer: 50 mM Tris-HCl pH 7.6, 2 mM DTT and 5 mM CaCl$_2$) was mixed with purified HA-tagged proteins for 16 h at 50 °C. After samples were boiled for 5 min, the peptide was purified by using Ni-agarose beads and was subjected to Dot blot and citrullination assays. Anti-histidine mAb (1/200) (Invitrogen Life Technologies) was used to detect Histidine in Dot blot assays.

2.11. Real time PCR

Cultured *wild-type* and transgenic trophozoites were homogenized in Trizol reagent (Invitrogen Life Technologies) and stored at −80 °C before total RNA extractions, according to the manufacturer's protocol. RNA was treated with DNase (Promega) before determination of nucleic acid concentration and cDNA synthesis with RevertAid™ Reverse Transcriptase (Fermentas). cDNA was analyzed for *wild-type* and transgenic trophozoite genes using real-time PCR SYBR Green Master Mix from Invitrogen (Invitrogen Life Technologies, Carlsbad, USA) single stranded cDNA (100 ng of the input total RNA equivalent), and 800 nM of amplification primer were used in a reaction volume of 20 μl. Specific primers were designed for detection of the *cwp1*, *cwp2*, *cwp3* and *gdh* genes: *cwp1*realF (AACGCTCTCACAGGCTCCAT) and *cwp1*realR (AGGTGGAGCTCCTTGAGAAATTG); *cwp2*realF (TAGGCTGCTTCCCACTTTTGAG) and *cwp2*realR (CGGGCCCGCAAGGT); *cwp3*realF (GCAAATTGGATGCCAAACAA) and *cwp3*realR (GACTCCGATCCAGTCGCAGTA). Runs were performed on a 7500 standard system (Applied Biosystems, USA). The relative-quantitative RT-PCR conditions were: 50 ºC for 2 min, 95 ºC for 10 min and 40 cycles at 95 ºC for 15 s and 60 ºC for 1 min. Gene expression was normalized to the housekeeping gene *gdh* (f: 5′AGGGCGGCTCCGACTTT 3′ and r: 5′ AGCGCATGACCTCGTTGTC 3′ primers) and calculated using the ΔΔCt method. Melt curve analyses were performed to ensure the specificity of the qPCR product. Statistical analysis was carried out using GraphPad Prism software (GraphPad Software, Inc.). The *t*-test was used to determine differences between *wild-type* cells (control group) and transgenic cells.

Fig. 4. Nuclear translocation of ADI depends on nuclear localization signals. A) Western blotting using anti-HA mAb in mutant forms of ADI (*mNLS1–mNLS3*) transgenic cells shows multiple bands. Presence of the 85 kDa band corresponding to the SUMOylated ADI form is observed in all mutant forms. Line 1: M$_r$: Relative Molecular Mass (kDa). B) Citrullination assay was performed by incubation of the His$_6$-CRGKA peptide with purified enzymes from the mutant forms of *mNLSs* transfected cells. ADI-HA purified enzyme was used as positive control and a non-related purified enzyme ESCP-HA was used as a negative control. Dot blotting to detect His$_6$-CcitGKA was performed using anti-citrulline (modified) antibody. The peptide His$_6$-CRGKA (or His$_6$-CCitGKA) was detected using anti-His mAb. C) Fluorescence analysis of parasites transfected with mutant forms of ADI (*mNLS1–mNLS3*) during encystation. Mutant ADI-HA proteins were labeled with Texas Red-conjugated anti-HA mAb; CWP1 was labeled with FITC-conjugated anti-CWP1 mAb. DIC: differential interference contrast images. Merged images and insets of DAPI staining of the nuclei are shown. Scale bar, 10 μm. D) Quantification of cells presenting nuclear transgenic ADI (presented as a percentage of total counted transfected cells) at 36 h after induction of the encystation process in *mNLS* transgenic trophozoites. Data represents the means ± s.d. of three independent experiments. E) Ratio between the number of nuclear transgenic ADI between *mNLS* mutant transgenic cells and *ADI-HA* trophozoites. Gray bars indicate the relative reduction compared with ADI-HA.

2.12. Structure modeling

As crystal structure for the ADI enzyme in *Giardia* is not available in Protein Data Bank, we used the web server Phyre2 [29] to predict ADI protein structure. We established the putative three dimensional localization of the SUMOylation motif (LKYE), defining the orientation of the Lys101 (or K101) residue. Three-dimensional structures were prepared using PyMol (DeLano Scientific, USA).
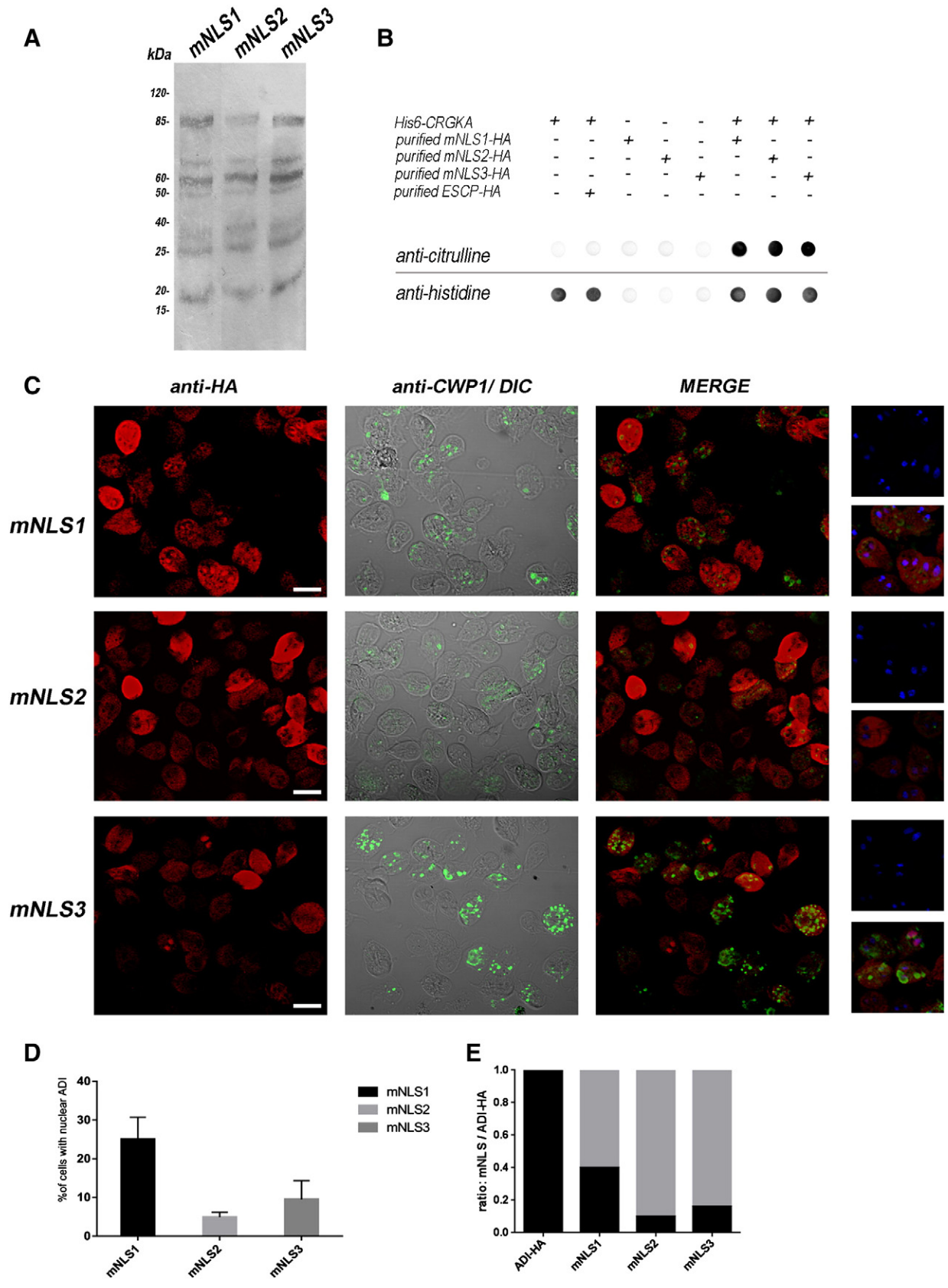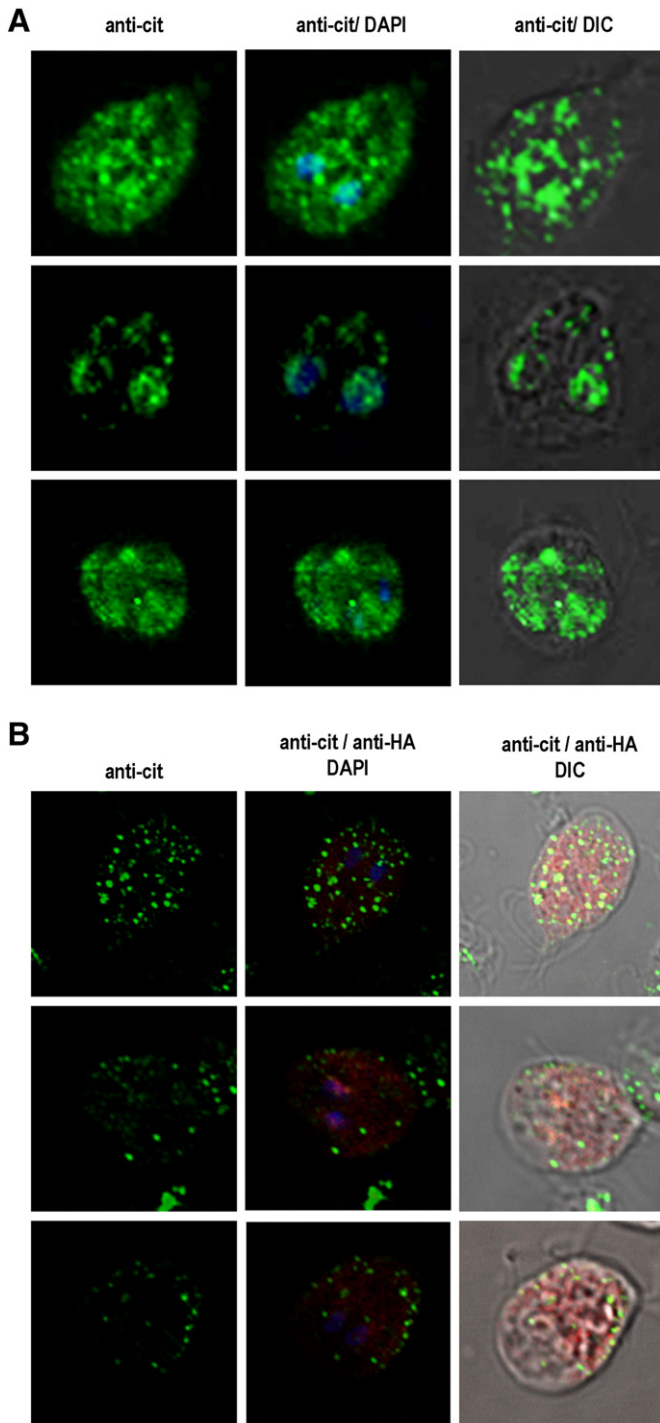
Fig. 5. Citrullination of histones during encystation. A) IFA and confocal microscopy using an anti-citrulline pAb in growing *wild-type* trophozoites (T), encysting cells (36 h; E) and cysts (C). Note the change of localization from cytoplasm to the nuclei during the differentiation process. Nuclei were stained with DAPI (blue). DIC (differential interference contrast) microscopy is shown. B) IFA and confocal microscopy on ADI_{K101A}-*HA* transgenic cells labeled with Texas Red-conjugated anti-HA mAb (red) and anti-citrulline pAb (green). Note absence of citrullination in the nuclei of ADI_{K101A}-*HA* transgenic cells. Nuclei were stained with DAPI (blue). DIC (differential interference contrast) microscopy is shown.

3. Results

3.1. Lysine residue 101 of ADI is the SUMOylation site

Some previous and independent experiments suggest that the SUMOylated form of ADI translocates to the nuclei during encystation.

By Western blot and immunoprecipitation assays, we previously demonstrated that the 85 kDa band corresponded to the SUMOylated form of ADI and was also present in the nuclear fraction of encysting trophozoites [5]. Moreover, we found that ADI cytoplasmic-to-nuclear relocalization occurred at the end of the cyst differentiation, when the encysting cells are full of ESVs [5].

These previous results prompted us to analyze the time-lapse of ADI and SUMO protein colocalization in the nuclei during encystation. For this, trophozoites overexpressing ADI (*ADI-HA*) were induced to encyst and tested using both anti-HA and a specific mAb raised against giardial SUMO [14]. Increased localization of ADI-HA and SUMO was observed in the nuclei during the encystation process, showing a peak between 24 and 36 h after induction of the encystation process but decreasing after that time (Fig. 1A). Quantitative colocalization analysis demonstrated partial colocalization between ADI-HA and SUMO (Fig. 1A, scatter plots). The scatter plots estimate the amount of fluorescence detected, based on localization of SUMO (red, y-axis) and ADI-HA (green, x-axis). Colocalized pixels (yellow) are located along the diagonal of the scatter gram. This partial colocalization was supported by the results of the Mander's (M) overlap coefficient, which was high at all times. The partial colocalization of both proteins is not surprising, taking into account that not all the ADI protein is SUMOylated and that there are many other proteins that might be modified by SUMO.

In order to confirm these results, trophozoites overexpressing SUMO (*SUMO-HA*) were tested using anti-HA mAb to detect SUMO-HA and a polyclonal antibody against ADI. Similar to the previous observation, the localization of ADI changed from the cytoplasm to the nuclear envelope, ending inside the nuclei as encystation progressed. Also, a clear co-localization with the SUMO-HA protein was observed with Mander's overlap coefficient, which varied between 0.8757 and 0.9985. Surprisingly, although *SUMO-HA* transgenic trophozoites did not show differences in the production of ESVs (Suppl. Fig. 1A), these transgenic cells were unable to produce cysts even 72 h post induction. Moreover, analysis of *SUMO-HA* encysting cells showed that there is no expression of CWP1 when SUMO-HA was highly expressed in the nuclei, co-localizing with ADI (Suppl. Fig. 1B, arrow). On the other hand, similar to what we have previously observed in *ADI-HA* transgenic cells, CWP1 is observed in *SUMO-HA* cells mildly expressing SUMO-HA (Suppl. Fig. 1B, arrowhead). These results suggest that SUMO is more available, either because the protein is overexpressed or because the HA tagging of SUMO disrupts its function and interaction with other cellular components. Therefore SUMO protein might be regulating the ADI function because, when SUMO protein is particularly accessible, ADI might have more chances of being SUMOylated and translocate to the nuclei early during encystation.

SUMO substrates show SUMOylation sites that follow a consensus motif with ψ-K-S-E/D (where ψ is a hydrophobic amino acid) [30–33]. We previously predicted two motifs with high probability as SUMOylation sites of ADI by using SUMOplot™ [5]. However, a number of more reliable programs for predicting SUMOylation sites are now available (e.g. SUMOsp 2.0 or PCI-SUMO), recognizing only the lysine 101 (K101) to be SUMOylated, with a prediction sensitivity of 89.12%. Analysis of the secondary structure using Phyre2 showed that this residue is located in a loop flanked by two helixes and the lysine is clearly exposed, as in most of the known SUMO target sites that fall either in unstructured N or C termini or in a loop region (Fig. 2A) [34, 35].

To experimentally examine if the K101 residue is the SUMOylated residue in ADI, a mutant lacking the putative SUMOylation site was generated from ADI. Before making the mutation of the K101 for alanine (A), and in order to predict if the mutation would affect ADI function, the SNAP method (developed by Yana Bromberg at Columbia University) was used. We found that the K101 mutation is "neutral" predicting that the resulting point-mutated protein is not functionally discernible from the native ADI. Therefore, the residue K101 was individually replaced by alanine (A) in the context of an expression vector encoding

ADI tagged with HA, and transfected trophozoites were generated (*ADI*$_{K101A}$-*HA*). When we used anti-HA mAb or an anti-ADI polyclonal antibody, we observed that the mutation did not change the cytoplasmic and flagellar localization (arrow) of the enzyme in growing (T) and encysting (E) *ADI*$_{K101A}$-*HA* transgenic trophozoites (Fig. 2B). Also, a minor portion of ADIK101A-HA was found in the nuclei in these encysting cells (see below). Quantitative colocalization analysis demonstrated a high degree of colocalization between ADI and *ADI*$_{K101A}$-*HA* (scatter plots on the right). The scatter plots indicate a yellow monopartite diagonal scatter pattern, which verifies the colocalization of both proteins, which is also supported by the results of the Mander's (M) overlap coefficient, which were 0.9985 and 0.9744, respectively. Conversely to cells overexpressing ADI-HA, anti-HA mAb did not detect the SUMOylated 85 kDa band in *ADI*$_{K101A}$-*HA* encysting cells by Western blotting (Fig. 2C). Also, we observed that there was a mild enrichment of the bands of low molecular weight in encysting *ADI*$_{K101A}$-*HA* cells. These results suggest that, in these cells, ADIK101A-HA was not SUMOylated and thus never expressed as an 85 kDa band. Another possibility is that the lower bands may correspond to degradation products of SUMOylated forms of the enzyme. To elucidate this, we performed immunoprecipitation assays using anti-SUMO mAb (13C5) in either *ADI-HA* or *ADI*$_{K101A}$-*HA* encysting cells (Fig. 2D). We found that anti-SUMO was able to immunoprecipitate the 85 kDa band of ADI-HA, confirming our previous results using a commercial antibody against SUMO1 [5]. However, neither the 85 kDa band nor bands of lower molecular weight were immunoprecipitated from *ADI*$_{K101A}$-*HA* cells, discarding the possibility that SUMOylated forms of ADI had been degraded. Taking into account that SUMO modification is related to protection of the proteins from degradation, it is possible that in this case, the absence of SUMOylation of ADI favors its partial degradation. To test the PAD activity of ADIK101A-HA, active ADIK101A-HA enzyme was purified from transgenic trophozoites using anti-HA antibody and, after incubation with the His$_6$-CRGKA peptide, was analyzed using anti-citrulline (modified) detection kit. After His$_6$-CRGKA purification and Dot blotting, we found that ADIK101A-HA, but not a non-related enzyme (ESCP), citrullinates the His$_6$-CRGKA peptide (Fig. 2E). ADI-HA purified enzyme was used as a positive control.

3.2. Nucleocytoplasmic shuttling of ADI partially depends on SUMOylation

When the *ADI*$_{K101A}$-*HA* transgenic trophozoites were induced to encyst and analyzed by IFA and confocal fluorescent microscopy 36 h after induction, a drastic reduction of ADIK101A-HA nuclear localization was observed compared with *ADI-HA* trophozoites (Fig. 3A and B) or *wild-type* trophozoites (not shown). This suggests that the SUMOylation of the enzyme promotes its translocation to the nuclei.

Using the anti-SUMO (13C5) mAb and the anti-HA mAb to detect ADIK101A-HA in IFA and confocal microscopy, no colocalization of these two proteins in *ADI*$_{K101A}$-*HA* transgenic encysting trophozoites was observed, indicating the lack of SUMOylation of *ADI*$_{K101A}$-*HA* (Fig. 3C). This was confirmed by the quantitative colocalization analysis showing a Mander's coefficient < 0.500 (Fig. 3C, right panels). Interestingly, even though a small number of cells showed ADIK101A-HA in the nuclei at 36 h post induction, there was no colocalization of this protein with SUMO (Fig. 3C, 36 h). Because the presence of ADI in the nuclei was dramatically reduced in *ADI*$_{K101A}$-*HA* transgenic encysting trophozoites, it became clear that nuclear translocation of ADI depends strongly, but not exclusively, on SUMOylation.

To track whether nuclear translocation of ADIK101A-HA occurs synchronically with the encystation, as was previously observed for ADI-HA and native ADI [5], a time-dependent analysis was performed in *ADI*$_{K101A}$-*HA* cells. Detailed analysis of the localization of ADIK101A-HA, together with the appearance of the CWP1, showed a progressive translocation of ADIK101A-HA toward nuclei during encystation in few cells, particularly when the encysting trophozoites were full of ESVs (Fig. 3D, 32–40 h). Nevertheless, the non-SUMOylated ADI (ADIK101A-HA) appeared in the nuclei of *ADI*$_{K101A}$-*HA* cells later during encystation when it was compared with the nuclear presence of ADI-HA in *ADI-HA* transgenic cells (Fig. 1A, 24 h). On the other hand, in the forming cyst, the localization of ADIK101A-HA in the nuclei decreased and no nuclear localization in the mature cyst was found (Fig. 3D, 48–56 h). All together, these results indicate that there is a shuttle of ADI between cytoplasm and nuclei during the encystation with SUMOylation improving the efficiency of nuclear localization. However, we cannot decipher if the impaired localization of ADIK101A-HA in the nuclei is because of a lower efficiency in nuclear import or if it is related to a failure in retention of the enzyme inside the nuclei. Moreover, although the SUMOylation of the ADI clearly promotes its movement to the nuclei, there may be other signals involved in the process.

### 3.3. Nuclear localization signals are critical for nuclear entry of ADI

Proteins destined for transport to the nucleus with a molecular mass higher than 50 kDa contain amino acid-targeting sequences called nuclear localization signals (NLSs). In order to find potential NLS sequences within ADI, bioinformatic analysis was performed using the PSORT II program (http://psort.nibb.ac.jp/form2.html). The results showed two putative NLSs in the ADI sequence: a conserved bipartite NLS, RRGIVMGQFQAPQRRREQ, which shows two basic residues (RR), 11 spacer residues and another basic region consisting of 3 basic residues (RRR), and a monopartite consensus sequence starting with proline and followed within 3 residues by a basic segment containing three arginine residues (PQRRREQ). Given that the bipartite consensus sequence consists of the monopartite consensus sequence plus a linker and upstream basic residues, all proteins containing a putative bipartite sequence also, by definition, contain a monopartite consensus sequence.

In an attempt to reveal whether the conserved NLSs in ADI are functional and are responsible for the entry of ADI into the nuclei, some mutations were constructed and their cellular localization was followed in transfected cells during encystations. Based on bioinformatic analysis, the amino acid mutations were designed taking into account their influence in the theoretical localization of the protein after the substitution for alanine (Table 1). To analyze if the mutation affects protein stability, cell lysates from *mNLS1–mNLS3* transgenic cells were analyzed by immunoblotting. Our results showed that the constructs showed the same pattern of protein bands, including the 85 kDa band corresponding to the SUMOylated form of ADI (Fig. 4A). To explore the PAD activity of the mutant constructs, a citrullination assay was performed using purified enzyme from the constructs and the His$_6$-CRGKA peptide. ADI-HA purified enzyme was used as a positive control. We found that all the constructs showed PAD activity (Fig. 4B).

All the substitutions made led to a diminished accumulation of ADI in the nuclei in encysting cells (after 36 h) compared with *ADI-HA* transgenic cells (Figs. 4C, D). However, substitution of the first two basic residues (R and R: *mNSL1*) with alanine residues at positions 181–182 in the first part of the conserved bipartite NLS resulted in a lower decrease compared with the other mutations (60%) (Fig. 4E). Substitution of valine and methionine (V and M: *mNSL2*) for alanine residues and substitution of proline for alanine in the first part of the monopartite NLS (P: *mNSL3*) showed a decrease of 90 and 85%, respectively, compared with *ADI-HA* transgenic cells. The results found in *mNLS1* and *mNLS3* transgenic cells matched the in silico prediction; however in *mNLS2* the shuttle to the nuclei would theoretically not be affected. These results suggest that both the bipartite and the monopartite NLSs are active sites involved in the entry of ADI to the nuclei and that mutations in other amino acids, despite basic residues, alter the entry of the protein to the nuclei.

Next, we introduced in ADI_{K101A}-HA transgenic cells, point mutations in the NLS sites described, in order to obtain double mutants to explore the subcellular localization of ADI. However, none of the transfection made in *Giardia* trophozoites produced viable cells, as occurred with other giardial proteins with expressions that are toxic for the cells [36].
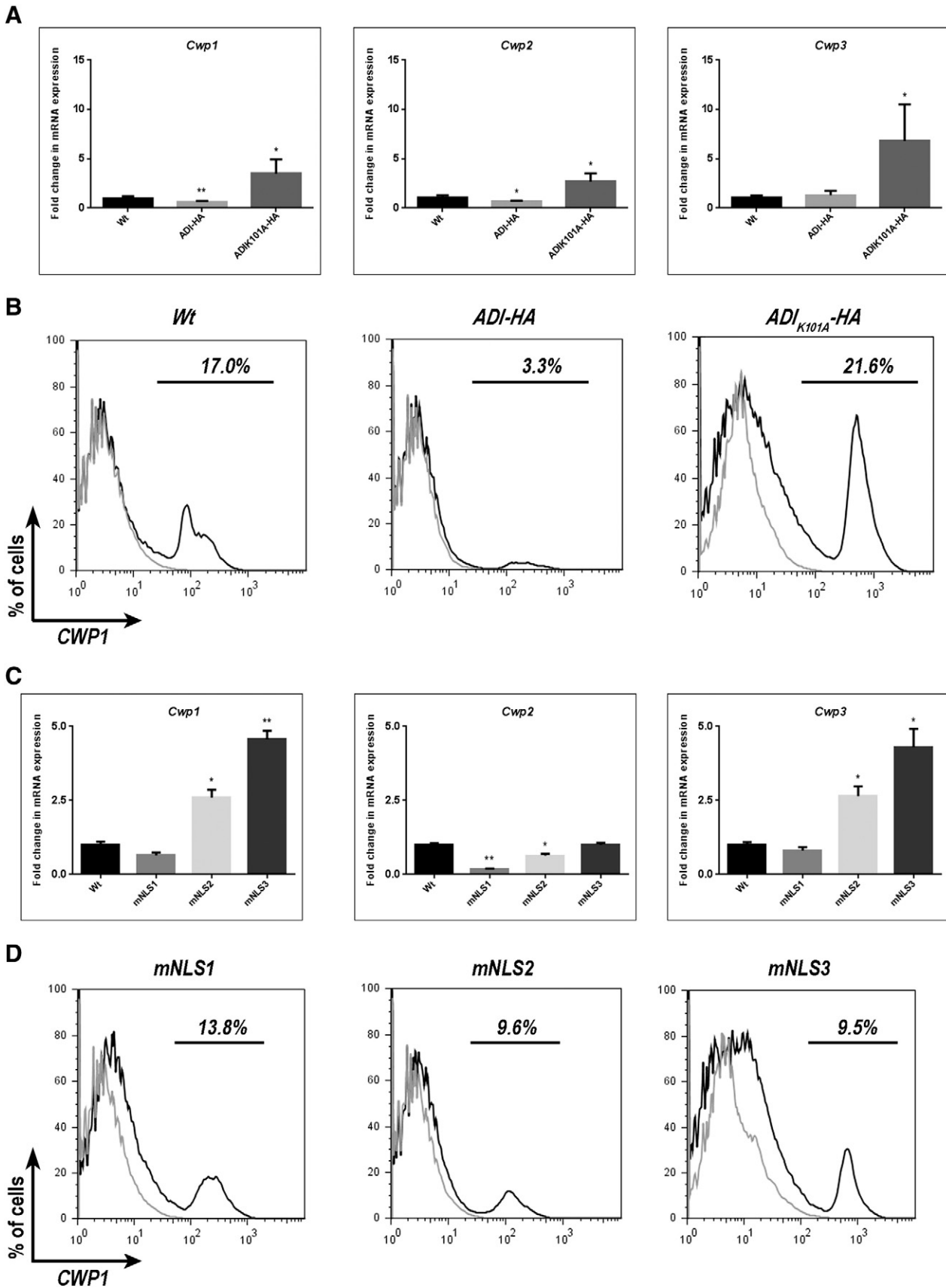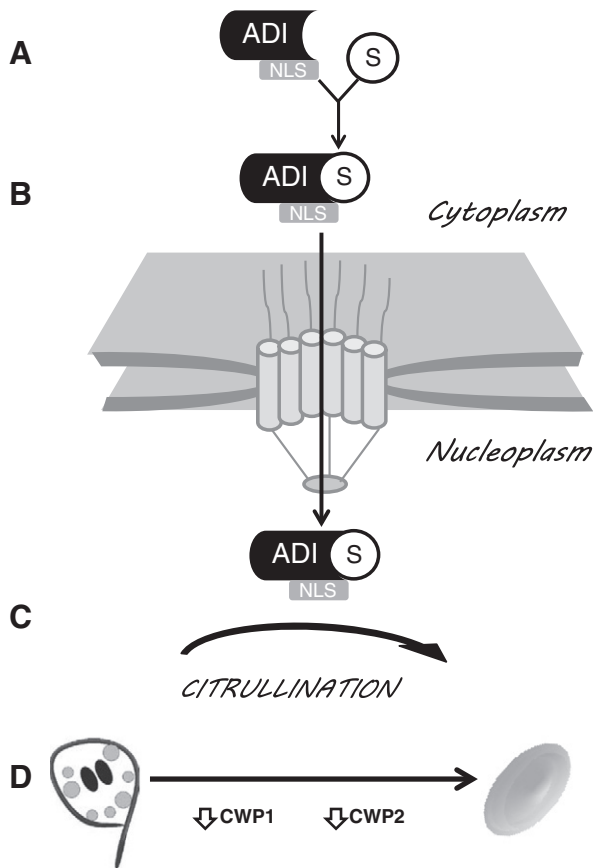
Fig. 7. Model of the translocation of ADI to the nuclei during encystation. During the differentiation process conjugation of ADI to the SUMO protein in the cytoplasm (A) seems to increase the efficiency of the translocation of the enzyme. (B) Nuclear localization signals are also involved. Inside the nuclei, ADI acts as a peptidyl arginine deiminase (C). As a consequence of ADI translocation, there is a downregulation of the expression of CWP1 and CWP2 proteins and cyst formation.

3.4. ADI acts as a PAD during encystation

Having demonstrated that ADI translocates to the nuclei during the encystation process, its function as a PAD within them (36 h after induction of encystation) was next evaluated. IFA and confocal microscopy using a modified anti-citrulline antibody revealed that the labeling changed during differentiation, from a cytoplasmic localization in *wild-type* trophozoites to a nuclear localization in encysting cells (Fig. 5A), still supporting the function of ADI as a PAD. The chromatin of both nuclei was labeled, as previously shown for the labeling of acetyl and methyl-modified histones [37,38]. When we analyzed citrullination in *ADI$_{K101A}$-HA* transfected cells, we found no citrullination in the nuclei, showing always a cytoplasmic pattern (Fig. 5B). As the whole, these results suggest that the translocation of ADI to the nuclei during encystation is related to its function as a PAD.

3.5. ADI regulates the production of mature cysts

As citrullination is known to modulate gene transcription, we performed qRT-PCR of *cwp* genes using mRNA extracted from *wild-type*, *ADI-HA* and *ADI$_{K101A}$-HA* transgenic trophozoites at 36 h of encystation. The mRNA levels of the endogenous *cwp1* and *cwp2* genes in the *ADI-HA* transgenic cells decreased ($p < 0.05$) relative to *wild-type* trophozoites (Fig. 6A). No significant changes were observed in *cwp3* gene. To further understand the function of giardial ADI, we observed the effect of over-expression of *ADI$_{K101A}$-HA* transgenic cells. We found that the levels of *cwp1*, *cwp2* and *cwp3* increased significantly compared with that of *wild-type* trophozoites during encystation. These results suggest a role of ADI in CWPs downregulation during the encystation process. In order to quantify the cysts within the total population of encysting cells, flow cytometry was performed using a mAb against CWP1 in non-permeabilized *wild-type* as well as in ADI transgenic trophozoites (Fig. 6B). The cells were not permeabilized in order to consider just the mature or forming cysts, which express CWP1 on the surface. As a control, a non-related antibody was used (gray line). The percentage of forming cysts was found to markedly decrease in *ADI-HA* transfected cells compared to *wild-type*. On the other hand, when cyst production was tested in *ADI$_{K101A}$-HA* transfected trophozoites, cyst production significantly increased compared to *ADI-HA* transfected trophozoites. This data provides evidence that suggest that SUMOylation and ADI translocation to the nuclei are probably related to the downregulation of proteins involved in the encystation process in *G. lamblia*.

To analyze if the impaired localization of *mNLS* transgenic cells in the nuclei is related to *cwp* gene expression, we performed qRT-PCR using mRNA from *mNLS* transgenic cells during encystation (Fig. 6C). We found that *cwp1* and *cwp3* gene expression showed and increased (*mNLS2* and *mNLS3*) or there were no differences (*mNLS1*) related to *wild-type* trophozoites. By contrast, *cwp2* gene expression showed a significant decrease (*mNLS1* and *mNLS2*) or no differences in *mNLS3*. When we analyzed the percentage of cyst produced by flow cytometry assays, we found that in all mutant transgenic cells, there were intermediate percentages of cysts between *ADI-HA* and *ADI$_{K101A}$-HA* encysting cells. It is important to note that in these *mNLS* transgenic trophozoites, SUMOylation of the enzyme takes place; therefore the enzyme that gets into the nuclei is still functional, explaining the partial downregulation of *cwp* genes in these mutant cells.

4. Discussion

G. lamblia encystation is a highly interesting biological process in which trophozoites perceive adverse conditions and unleash an organized process in which synthesis, accumulation and secretion of cyst wall components are critical steps. Despite considerable information at the cellular level, the basis of molecular mechanisms involved in the generation, regulation and downregulation of gene expression during encystation remains unclear. This study shows evidence related to the downregulation of *cwps* genes, in a process closely related to ADI translocation to the nuclei during encystation. Two types of protein posttranslational modifications were involved. One was the SUMOylation of ADI, which contributes to improve the efficiency of nuclear import or permanence of the enzyme inside the nuclei, and

Fig. 6. ADI downregulates the encystation process. A) Real-time PCR was performed using *cwp1-3* gene-specific primers in *wild-type*, *ADI-HA* and *ADI$_{K101A}$-HA* transgenic cells, 36 h after induction of encystation. Fold changes in mRNA expression are shown as the ratio of transcript levels in *mNLS* transgenic cells relative to *wild-type* trophozoites. Expression was normalized to that of *gdh*. Each sample was loaded in triplicate and experiments were repeated at least three times. The data was statistically evaluated using Student's *t* test, *$p < 0.05$. B) Flow cytometry assays were performed on non-permeabilized encysting *wild-type* trophozoites (Wt), *ADI-HA* or *ADI$_{K101A}$-HA* transgenic trophozoites using anti-CWP1 mAb (x axis). Overlay histograms show the result of an unrelated antibody (gray). Percentage of positive cells (cysts) is indicated. C) Quantitative real time PCR analysis of gene expression in *mNLS* transgenic cells 36 h after induction of the encystation process. The assay was performed using primers specific for *cwp1-3* genes. Transcript levels were normalized to *gdh* RNA levels. Fold changes in mRNA expression are shown as the ratio of transcript levels in *mNLS* transgenic cells relative to *wild-type* (Wt) trophozoites. Experiments were repeated at least three times, and data was statistically evaluated using Student's *t* test, *$p < 0.05$. D) Flow cytometry assays performed in non-permeabilized *mNLS* transgenic cells 36 h after induction of encystation using anti CWP1 mAb (x axis). Overlay histograms show the result of an unrelated antibody (gray). Percentage of positive cells (cysts) is indicated.

the other is the citrullination of nuclear proteins resulting from the function of ADI as a PAD in the nuclei. These results provide insights into possible pathways by which ADI participates during stage differentiation in this protozoan parasite.

Since the discovery of the protein modifier SUMO about 16 years ago, much has been learned about the enzymatic system mediating SUMO conjugation and deconjugation in eukaryotic cells. Also, the number of proteins identified as substrates of SUMO modification is rapidly increasing. However, much remains to be understood about how SUMOylation modifies the functions of these proteins [39]. While many questions remain unresolved in more evolved cells, the situation is even more unclear in parasites. The SUMO conjugation system has been described in *Toxoplasma gondii*, *Plasmodium falciparum*, *Trypanosoma cruzi*, *Schistosoma mansoni* and *G. lamblia* [14,40–43]. Many of these studies are just descriptive of the enzymes involved in the SUMO cycle and, in only a few cases, the SUMO substrates have been established. Still, the biological role of SUMO conjugation in parasites remains to be elucidated.

Recently, it has been demonstrated that paraflagellar rod protein (PFR1) is a flagellar substrate of SUMO in *T. cruzi* and may play a role in differentiation of *T. cruzi* [44]. Our studies also showed that the enzyme ADI is a SUMOylated enzyme in *G. lamblia* [5], and that ADI is specifically SUMOylated on Lys101, inside a typical SUMOylation motif that is not part of a helix according to the secondary structure prediction. The described enzymes of the SUMOylation pathway are both in the cytoplasm and surrounding the nuclei [14], and so SUMOylation of ADI may take place either in the cytoplasm or in the perinuclear region. Our results indicate that SUMOylation of ADI improved nuclear import efficiency during encystation, as was suggested to be one of the functions of SUMO conjugation in other cells [45–47]. However, in eukaryotic cells, the best understood pathway of nuclear-cytoplasmic transport is a classic nuclear import pathway, where proteins that crisscross the nuclear membrane contain a stretch of basic amino acid sequence: the NLSs. ADI shows both a monopartite and a bipartite putative NLSs, and they were found to be involved in the translocation of the enzyme to the nuclei. Proteins with NLSs are transported across the nuclear envelope by a family of transport proteins called karyopherins or importins. In the *Giardia* genome data base, only the importin β-3 subunit (GL50803_15106) is described. It shows the HEAT domain involved in intracellular transport and contains a domain with high probability of SUMO interaction. The involvement of this importin in ADI transport across the nuclear membrane is a matter of ongoing experiment. Interestingly, it is known that nuclear-cytoplasmic transport modulated by posttranslational modification of the cargo protein, including SUMOylation, could mask or expose the NLS of the protein. We found that ADI shuttle to the nuclei even in the absence of SUMOylation of the enzyme, but the localization of the enzyme in the nuclei is higher when ADI is SUMOylated. These results may be explained taking into account the molecular consequences of SUMOylation. One possible explanation is that SUMOylation keeps the enzyme inside the nuclei, as was demonstrated in other cells [48]. Another possibility is that the SUMOylation of ADI may lead to a conformational change in ADI, which now exposes the NLS or the site where it is bonded to importin β. It will be interesting to further explore if there is an association of the SUMOylated form of ADI with importins, or with other cargo proteins, in order to crisscross the nuclear membrane.

We have previously demonstrated that the enzyme ADI, besides its role as a metabolic enzyme, acts as a PAD during the antigenic variation process [5]. Here, using an antibody against modified citrulline, we found that the enzyme was able to deiminate arginine residues within nuclear proteins during encystation. However, using this detection method, it is possible to determine the citrullination state of an entire protein without being able to identify the protein or annotate the location of the converted arginine. In eukaryotic cells, PAD4 has been described as being recruited to the promoters of numerous genes producing the deimination (citrullination) of the histones H3 and H4, with this modification being associated with the decreased

transcription level of those genes via an unknown mechanism [49]. This suggested that the ADI enzyme might be able to deiminate histones during the encystation of *G. lamblia*. In preliminary studies, we purified nuclear proteins from growing and encysting cells and after MALDI-ToF-MS analysis we identified histone H4, histone H2A and histone H2B. Using the anti-citrulline (modified) antibody and Western blotting assay, we found citrullinated proteins identifiable in the 11–16 kDa region, matching the predicted masses of histone proteins in encysting cells. Although this result suggests histone citrullination, complementary experiments are needed to confirm the presence of citrullinated histones during encystation. In *Giardia*, very little is known about epigenetic modifications of histones. Lysine methylation has been suggested in histone H3, but arginine methylation has not been studied yet. Unraveling the importance of posttranslational modification of nuclear proteins will undoubtedly bring forth new knowledge to the field of epigenetic regulation of gene expression in *Giardia*.

Given that the relocalization of ADI from the cytoplasm to the nucleus depends on the differentiation of the parasite, it is possible that a cascade of events is involved in this mechanism. Although it has been observed that the lack of cholesterol triggers the encystation process, it is not known how cholesterol deprivation initiates specific gene regulation. In the upregulation of encystation gene expression, several transcriptional factors have been identified, such as Myb-2 [50,51], GARP [52], WRKY [53], E2F [54], AT-rich interaction domain (ARID) [55], and recently Pax proteins (1 and 2) [56]. All these transcription factors are involved in the upregulation of *cwp* genes and therefore involved in *cwp* gene regulation during encystation. However, as the encystation process progresses, there may also be signals to downregulate *cwp* expression. We suggest that the enzyme ADI is involved in this process, because in ADI mutants in which SUMOylation is absent (ADI_{K101A}-HA trophozoites) and translocation to the nuclei is diminished, the quantity of cysts produced is higher than in *ADI-HA* transfected cells. We therefore may draw a model in which there would be a coordinated cascade of events (Fig. 7). The first signal that drives ADI to the nuclei would be the SUMOylation of the enzyme which probably exposes NLS signals promoting the entry of the enzyme to the nuclei. Once inside the nuclei, ADI acts as a PAD and, by an unknown mechanism, induces the downregulation of *cwp* genes, allowing the encystation process to end. Our results therefore establish an important integration point for two protein-modifying pathways in *Giardia*, in which SUMOylation and deimination converge as key players in the regulation of cyst production in this parasite.

Supplementary data to this article can be found online at http://dx.doi.org/10.1016/j.bbamcr.2014.04.014.

Acknowledgments

References

[1] D.B. Huang, A.C. White, An updated review on *Cryptosporidium* and *Giardia*, Gastroenterol. Clin. North. Am. 35 (2006) 291–314 (viii).
[2] R.D. Adam, Biology of *Giardia lamblia*, Clin. Microbiol. Rev. 14 (2001) 447–475.
[3] S.G. Svard, P. Hagblom, J.E. Palm, *Giardia lamblia* — a model organism for eukaryotic cell differentiation, FEMS Microbiol. Lett. 218 (2003) 3–7.
[4] E.R. Vossenaar, A.J. Zendman, W.J. van Venrooij, G.J. Pruijn, PAD, a growing family of citrullinating enzymes: genes, features and involvement in disease, Bioessays 25 (2003) 1106–1118.
[5] M.C. Touz, A.S. Ropolo, M.R. Rivero, C.V. Vranych, J.T. Conrad, S.G. Svard, T.E. Nash, Arginine deiminase has multiple regulatory roles in the biology of *Giardia lamblia*, J. Cell Sci. 121 (2008) 2930–2938.
[6] E. Ringqvist, J.E. Palm, H. Skarin, A.B. Hehl, M. Weiland, B.J. Davids, D.S. Reiner, W.J. Griffiths, L. Eckmann, F.D. Gillin, S.G. Svard, Release of metabolic enzymes by *Giardia* in response to interaction with intestinal epithelial cells, Mol. Biochem. Parasitol. 159 (2) (2008) 85–91.
[7] A.S. Ropolo, M.C. Touz, A lesson in survival, by *Giardia lamblia*, Sci. World J. 10 (2010) 2019–2031.

[8] S. Banik, P. Renner Viveros, F. Seeber, C. Klotz, R. Ignatius, T. Aebischer, *Giardia duodenalis* arginine deiminase modulates the phenotype and cytokine secretion of human dendritic cells by depletion of arginine and formation of ammonia, Infect. Immun. 81 (2013) 2309–2317.

[9] B. Stadelmann, M.C. Merino, L. Persson, S.G. Svard, Arginine consumption by the intestinal parasite *Giardia intestinalis* reduces proliferation of intestinal epithelial cells, PLoS ONE 7 (2012) e45325.

[10] B. Stadelmann, K. Hanevik, M.K. Andersson, O. Bruserud, S.G. Svard, The role of arginine and arginine-metabolizing enzymes during *Giardia* — host cell interactions in vitro, BMC Microbiol. 13 (2013) 256.

[11] Z. Li, L. Kulakova, L. Li, A. Galkin, Z. Zhao, T.E. Nash, P.S. Mariano, O. Herzberg, D. Dunaway-Mariano, Mechanisms of catalysis and inhibition operative in the arginine deiminase from the human pathogen *Giardia lamblia*, Bioorg. Chem. 37 (2009) 149–161.

[12] J. Anckar, L. Sistonen, SUMO: getting it on, Biochem. Soc. Trans. 35 (2007) 1409–1413.

[13] R. Geiss-Friedlander, F. Melchior, Concepts in sumoylation: a decade on, Nat. Rev. Mol. Cell Biol. 8 (2007) 947–956.

[14] C.V. Vranych, M.C. Merino, N. Zamponi, M.C. Touz, A.S. Rópolo, SUMOylation in *Giardia lamblia*: A conserved post-translational modification in one of the earliest divergent eukaryotes, Biomolecules 2 (2012) 312–330.

[15] D.B. Keister, Axenic culture of *Giardia lamblia* in TYI-S-33 medium supplemented with bile, Trans. R. Soc. Trop. Med. Hyg. 77 (1983) 487–488.

[16] S.M. Singer, J. Yee, T.E. Nash, Episomal and integrated maintenance of foreign DNA in *Giardia lamblia*, Mol. Biochem. Parasitol. 92 (1998) 59–69.

[17] J. Yee, T.E. Nash, Transient transfection and expression of firefly luciferase in *Giardia lamblia*, Proc. Natl. Acad. Sci. U. S. A. 92 (1995) 5615–5619.

[18] S.E. Boucher, F.D. Gillin, Excystation of in vitro-derived *Giardia lamblia* cysts, Infect. Immun. 58 (1990) 3516–3522.

[19] J. Ren, X. Gao, C. Jin, M. Zhu, X. Wang, A. Shaw, L. Wen, X. Yao, Y. Xue, Systematic study of protein sumoylation: development of a site-specific predictor of SUMOsp 2.0, Proteomics 9 (2009) 3409–3412.

[20] M.C. Touz, H.D. Lujan, S.F. Hayes, T.E. Nash, Sorting of encystation-specific cysteine protease to lysosome-like peripheral vacuoles in *Giardia lamblia* requires a conserved tyrosine-based motif, J. Biol. Chem. 278 (2003) 6420–6426.

[21] H.G. Elmendorf, S.M. Singer, T.E. Nash, The abundance of sterile transcripts in *Giardia lamblia*, Nucleic Acids Res. 29 (2001) 4674–4683.

[22] M.C. Touz, L. Kulakova, T.E. Nash, Adaptor protein complex 1 mediates the transport of lysosomal proteins from a Golgi-like organelle to peripheral vacuoles in the primitive eukaryote *Giardia lamblia*, Mol. Biol. Cell 15 (2004) 3053–3060.

[23] M.C. Touz, J.T. Conrad, T.E. Nash, A novel palmitoyl acyl transferase controls surface protein palmitoylation and cytotoxicity in *Giardia lamblia*, Mol. Microbiol. 58 (2005) 999–1011.

[24] V. Zinchuk, O. Zinchuk, T. Okada, Quantitative colocalization analysis of multicolor confocal immunofluorescence microscopy images: pushing pixels to explore biological phenomena, Acta Histochem. Cytochem. 40 (2007) 101–111.

[25] P. Garcia Penarrubia, X. Ferez Ruiz, J. Galvez, Quantitative analysis of the factors that affect the determination of colocalization coefficients in dual-color confocal images, IEEE Trans. Image Process. 14 (2005) 1151–1158.

[26] H. Sun, W.J. Crossland, Quantitative assessment of localization and colocalization of glutamate, aspartate, glycine, and GABA immunoreactivity in the chick retina, Anat. Rec. 260 (2000) 158–179.

[27] C. Zhu, R.J. Barker, A.W. Hunter, Y. Zhang, J. Jourdan, R.G. Gourdie, Quantitative analysis of ZO-1 colocalization with Cx43 gap junction plaques in cultures of rat neonatal cardiomyocytes, Microsc. Microanal. 11 (2005) 244–248.

[28] T. Senshu, K. Akiyama, S. Kan, H. Asaga, A. Ishigami, M. Manabe, Detection of deiminated proteins in rat skin: probing with a monospecific antibody after modification of citrulline residues, J. Investig. Dermatol. 105 (1995) 163–169.

[29] L.A. Kelley, M.J. Sternberg, Protein structure prediction on the Web: a case study using the Phyre server, Nat. Protoc. 4 (2009) 363–371.

[30] C. Denison, A.D. Rudner, S.A. Gerber, C.E. Bakalarski, D. Moazed, S.P. Gygi, A proteomic strategy for gaining insights into protein sumoylation in yeast, Mol. Cell. Proteomics 4 (2005) 246–254.

[31] R.T. Hay, SUMO: a history of modification, Mol. Cell 18 (2005) 1–12.

[32] E.S. Johnson, Protein modification by SUMO, Annu. Rev. Biochem. 73 (2004) 355–382.

[33] F. Melchior, M. Schergaut, A. Pichler, SUMO: ligases, isopeptidases and nuclear pores, Trends Biochem. Sci. 28 (2003) 612–618.

[34] C. Hoege, B. Pfander, G.L. Moldovan, G. Pyrowolakis, S. Jentsch, RAD6-dependent DNA repair is linked to modification of PCNA by ubiquitin and SUMO, Nature 419 (2002) 135–141.

[35] V. Bernier-Villamor, D.A. Sampson, M.J. Matunis, C.D. Lima, Structural basis for E2-mediated SUMO conjugation revealed by a complex between ubiquitin-conjugating enzyme Ubc9 and RanGAP1, Cell 108 (2002) 345–356.

[36] M.R. Rivero, L. Kulakova, M.C. Touz, Long double-stranded RNA produces specific gene downregulation in *Giardia lamblia*, J. Parasitol. 96 (2010) 815–819.

[37] S.C. Dawson, M.S. Sagolla, W.Z. Cande, The cenH3 histone variant defines centromeres in *Giardia intestinalis*, Chromosoma 116 (2007) 175–184.

[38] S. Sonda, L. Morf, I. Bottova, H. Baetschmann, H. Rehrauer, A. Caflisch, M.A. Hakimi, A.B. Hehl, Epigenetic mechanisms regulate stage differentiation in the minimized protozoan *Giardia lamblia*, Mol. Microbiol. 76 (2010) 48–67.

[39] R.J. Dohmen, SUMO protein modification, Biochim. Biophys. Acta 1695 (2004) 113–131.

[40] N. Issar, E. Roux, D. Mattei, A. Scherf, Identification of a novel post-translational modification in *Plasmodium falciparum*: protein sumoylation in different cellular compartments, Cell. Microbiol. 10 (2008) 1999–2011.

[41] L. Braun, D. Cannella, A.M. Pinheiro, S. Kieffer, H. Belrhali, J. Garin, M.A. Hakimi, The small ubiquitin-like modifier (SUMO)-conjugating system of *Toxoplasma gondii*, Int. J. Parasitol. 39 (2009) 81–90.

[42] R.V. Pereira, F.J. Cabral, M.S. Gomes, E.H. Baba, L.K. Jannotti-Passos, O. Carvalho, V. Rodrigues, R.J. Afonso, W. Castro-Borges, R. Guerra-Sa, Molecular characterization of SUMO E2 conjugation enzyme: differential expression profile in *Schistosoma mansoni*, Parasitol. Res. 109 (2011) 1537–1546.

[43] J.C. Bayona, E.S. Nakayasu, M. Laverriere, C. Aguilar, T.J. Sobreira, H. Choi, A.I. Nesvizhskii, I.C. Almeida, J.J. Cazzulo, V.E. Alvarez, SUMOylation pathway in *Trypanosoma cruzi*: functional characterization and proteomic analysis of target proteins, Mol. Cell. Proteomics 10 (2011) (M110 007369).

[44] T. Annoura, T. Makiuchi, I. Sariego, T. Aoki, T. Nara, SUMOylation of paraflagellar rod protein, PFR1, and its stage-specific localization in *Trypanosoma cruzi*, PLoS ONE 7 (2012) e37183.

[45] U. Rothenbusch, M. Sawatzki, Y. Chang, S. Caesar, G. Schlenstedt, Sumoylation regulates Kap114-mediated nuclear transport, EMBO J. 31 (2012) 2461–2472.

[46] Q. Cai, E.S. Robertson, Ubiquitin/SUMO modification regulates VHL protein stability and nucleocytoplasmic localization, PLoS ONE 5 (2010).

[47] K.J. Miranda, R.F. Loeser, R.R. Yammani, Sumoylation and nuclear translocation of S100A4 regulate IL-1beta-mediated production of matrix metalloproteinase-13, J. Biol. Chem. 285 (2010) 31517–31524.

[48] F. Renner, R. Moreno, M.L. Schmitz, SUMOylation-dependent localization of IKKepsilon in PML nuclear bodies is essential for protection against DNA-damage-triggered cell death, Mol. Cell 37 (2010) 503–515.

[49] Y. Wang, J. Wysocka, J. Sayegh, Y.H. Lee, J.R. Perlin, L. Leonelli, L.S. Sonbuchner, C.H. McDonald, R.G. Cook, Y. Dou, R.G. Roeder, S. Clarke, M.R. Stallcup, C.D. Allis, S.A. Coonrod, Human PAD4 regulates histone arginine methylation levels via demethylimination, Science 306 (2004) 279–283.

[50] C.H. Sun, D. Palm, A.G. McArthur, S.G. Svard, F.D. Gillin, A novel Myb-related protein involved in transcriptional activation of encystation genes in *Giardia lamblia*, Mol. Microbiol. 46 (2002) 971–984.

[51] Y.C. Huang, L.H. Su, G.A. Lee, P.W. Chiu, C.C. Cho, J.Y. Wu, C.H. Sun, Regulation of cyst wall protein promoters by Myb2 in *Giardia lamblia*, J. Biol. Chem. 283 (2008) 31021–31029.

[52] C.H. Sun, L.H. Su, F.D. Gillin, Novel plant-GARP-like transcription factors in *Giardia lamblia*, Mol. Biochem. Parasitol. 146 (2006) 45–57.

[53] Y.J. Pan, C.C. Cho, Y.Y. Kao, C.H. Sun, A novel WRKY-like protein involved in transcriptional activation of cyst wall protein genes in *Giardia lamblia*, J. Biol. Chem. 284 (2009) 17975–17988.

[54] L.H. Su, Y.J. Pan, Y.C. Huang, C.C. Cho, C.W. Chen, S.W. Huang, S.F. Chuang, C.H. Sun, A novel E2F-like protein involved in transcriptional activation of cyst wall protein genes in *Giardia lamblia*, J. Biol. Chem. 286 (2011) 34101–34120.

[55] C.H. Wang, L.H. Su, C.H. Sun, A novel ARID/Bright-like protein involved in transcriptional activation of cyst wall protein 1 gene in *Giardia lamblia*, J. Biol. Chem. 282 (2007) 8905–8914.

[56] S.F. Chuang, L.H. Su, C.C. Cho, Y.J. Pan, C.H. Sun, Functional redundancy of two Pax-like proteins in transcriptional activation of cyst wall protein genes in *Giardia lamblia*, PLoS ONE 7 (2012) e30614